Presented at the 35th PVSC, June 20-25, 2010, Honolulu, Hawaii

MODELING OF THE DEGRADATION OF III-V TRIPLE-JUNCTION CELLS DUE TO PARTICLE IRRADIATION ON THE BASIS OF COMPONENT CELLS

C. Baur[1], A. W. Bett[2]
[1]European Space Agency, Noordwijk, The Netherlands
[2]Fraunhofer Institute for Solar Energy Systems, Freiburg, Germany

ABSTRACT

The paper reports about the possibility of predicting the degradation of III-V multi-junction solar cells due to particle irradiation in space solely based on the radiation response of the respective sub cells. State-of-the art triple-junction solar cells of the 3G28 class manufactured by AZUR Space GmbH are used as an example to demonstrate how to model the degradation behavior of multi-junction cell from the degradation behavior of the respective component cells, as investigated in this study. The advantages of component cells for understanding and modeling the behavior of multi-junction cells under different conditions are discussed.

INTRODUCTION

An accurate prediction of solar cell degradation in space due to particle irradiation is one of the major prerequisites for an optimized sizing of the solar generator. With the introduction of multi-junction solar cells the prediction of this performance degradation reached a higher level of complexity. Although, there are nowadays models in place (e.g. [1,2]) which allow for a reasonable degradation prediction of state-of-the-art triple-junction (3J) cells, these models were initially developed for single-junction solar cells and as such typically treat multi-junction cells as a single-junction cell. This might be in most cases and applications a sufficient approximation; however, from a physical point of view this is not justified. In this paper an approach is chosen which aims for basing the deduction of solar cell degradation due to particle irradiation on fundamental solar cell physics. Eventually, the 3J cell degradation is modeled using the individual degradation behavior of each sub cell within the 3J cell. Hence, the base is the investigation of component cells which are single-junction cells being composed of almost the same layer structure as the corresponding 3J cell but with only one semiconductor material being electrically active. Thus, it can be assumed that component cells have identical optical and electrical properties as the corresponding sub cells in the 3J cell. Being single-junction cells, component cells have the advantage over 3J cells that the individual cell properties including the radiation response are fully accessible.

The approach to base solar cell degradation on fundamental solar cell physics is not new. A lot of research has been done over the last years in this respect [3,4]. However, the models having evolved from these approaches have in common that as inputs to the models very detailed information about the semiconductor materials (e.g. doping levels) and geometries of the cell structure (thicknesses of emitter and base) are required which are typically proprietary information of the solar cell manufacturers. This is in contrast to the approach introduced in this paper where no detailed background information on the cell structure is needed.

EXPERIMENT

In this study, triple-junction (3J) solar cells of the 3G28% type by AZUR Space GmbH and corresponding component cells were characterized at beginning of life (BOL) and after electron and proton irradiation of different energies and fluences. An overview of the particles, energies and fluence ranges applied is given in Table 1. Proton irradiations were performed at the Commissariat à l'énergie atomique (CEA) in Paris, while electron irradiation was carried out at the Delft University of Technology (TU Delft) in the Netherlands.

particle	Energy [MeV]	Fluence range [cm^{-2}]
electrons	1	$1{\cdot}10^{14}$ - $1{\cdot}10^{16}$
electrons	3	$5{\cdot}10^{13}$ - $5{\cdot}10^{15}$
protons	4	$1{\cdot}10^{11}$ – $3{\cdot}10^{12}$
protons	5	$5{\cdot}10^{10}$ - $1{\cdot}10^{12}$
protons	8.2	$5{\cdot}10^{10}$ - $2{\cdot}10^{12}$

Table 1 Particles, energies and fluence ranges used in the irradiation experiments.

The characterization of the solar cells included the measurement of external quantum efficiencies, light and dark I-V characteristics in order to determine the degradation characteristics of the cells. It should be noted that all cells were 2x2 cm^2 cells. Nevertheless, it has been verified that all results presented here are applicable to standard size cells (4x8 cm^2 with cropped corners) as well [5]. The purpose of the additional irradiation experiments on component cells was to get a better understanding of the 3J cell degradation and to demonstrate that it is possible to derive the degradation characteristic of the 3J cell from the degradation characteristics of the respective component cells.

RESULTS

Comparison of 3J and component cells

As a first step it has to be demonstrated that component cells indeed have the same optical and electrical properties as sub cells in the 3J cell. Since component

cells and 3J cells differ slightly in the internal structure i.e. different doping, this cannot be taken for granted a priori.
From the comparison of external quantum efficiency (EQE) measurements optical and electrical differences can be easily seen.
Figure 1 shows the EQE measurements of a 3J cell and corresponding component cells BOL (upper graph) and after irradiation with 4 MeV protons at a fluence of $3{\cdot}10^{12}$ cm^{-2} (lower graph). After irradiation the measurements of the sub cells and the component cells are in very good agreement. There are only slight differences in the interference pattern which can be attributed to slightly different optical properties between 3J and component cells. This in turn is the result from the differences in the cell structures. At BOL the top and the middle cell measurements are also in good agreement. However, the bottom component cell shows a large signal in a wavelength region where the GaInAs layer should have absorbed all the photons.

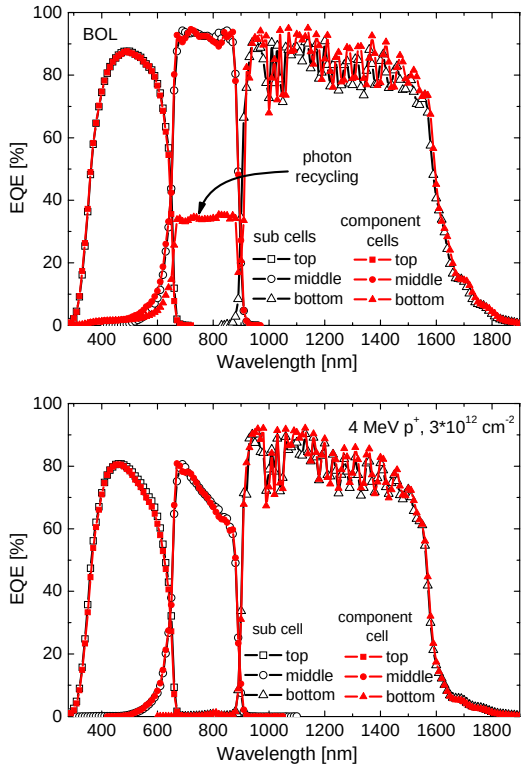

Figure 1 EQE of a 3J cell and component cells BOL (upper graph) and after irradiance with 4 MeV protons at a fluence of $3{\cdot}10^{12}$ cm^{-2} (lower graph). Except for the bottom cell at BOL the EQE measurements of the sub cells and the corresponding component cells are in very good agreement.

In fact the photons are absorbed in the upper layers but due to photon recycling effects reemitted photons can reach the active Ge layer. This phenomenon is described in detail in [6] where also a correction procedure is given taking the photon recycling effect into account.

Modeling approach

The fundamental equation used for the modeling of solar cells and their degradation is the two diode model (e.g. [7]):

$$I(V) = I_{01}\left(e^{\left(\frac{qV-R_S}{k_BT}\right)}-1\right) + I_{02}\left(e^{\left(\frac{qV-R_S}{2k_BT}\right)}-1\right) - I_{photo} + \frac{V-IR_S}{R_P} \quad (1)$$

where I is the cell current, V the cell voltage, I_{photo} the photocurrent, I_{01} and I_{02} the dark saturation currents, R_S and R_P the serial and parallel resistances, q the elementary charge, k_B the Boltzmann constant and T the temperature. The diode quality factors have been set to 1 and 2 respectively as can be seen in the exponential expressions. All single-junction cells (i.e. all component cells) investigated in this study are modeled by Eq. (1).
The attractiveness of the two diode model is given by the fact that the parameters are accessible relatively easy by non-elaborate measurements. Except for the photocurrent all parameters can be derived from fitting Eq. (1) (without I_{photo}) to dark I-V measurements of the solar cells.

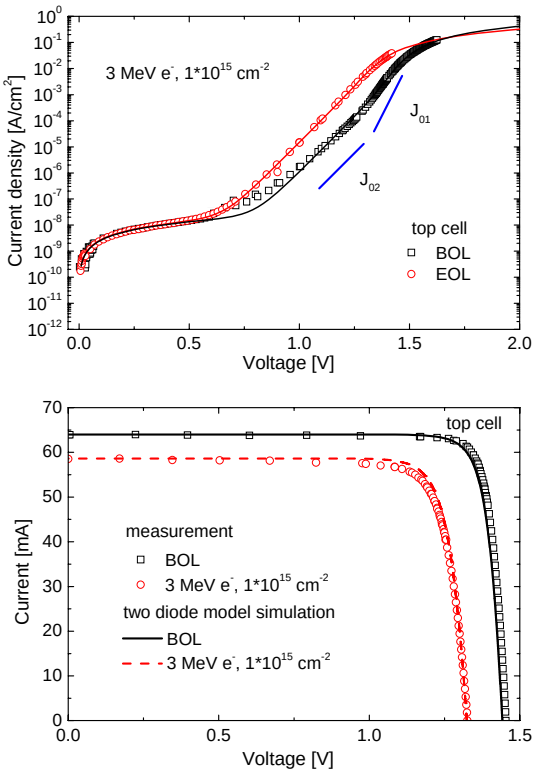

Figure 2 Dark and light I-V characteristics of a GaInP component cell. Open symbols are measured data while lines are fitting curves (upper graph) or the results of the modeling process (lower graph).

I_{photo} can either be derived from direct measurements of the I-V curve making the (in most cases) valid assumption that I_{SC} = I_{photo} or by measuring the spectral response of the cells in absolute terms and integrate with the AM0 spectrum.
That this approach results in a reasonable agreement between measured data and simulation is demonstrated in Fig. 2. In the upper graph of Fig. 2 the dark I-V curve of a top component cell is shown BOL and after irradiation with 3 MeV electrons and a fluence of $1 \cdot 10^{15}$ cm^{-2}. The lines in the upper graph are the result of least square fits to the measured data using Eq. (1) (without I_{photo}). In the lower graph of Fig. 2 the I-V curve of the same top component cell is shown measured under the AM0 spectrum (symbols) and when simulated using the two diode model (lines). The necessary parameters to be fed into the model were derived from the fitting process to the dark I-V curve while I_{photo} was identical to the light I-V I_{SC}.

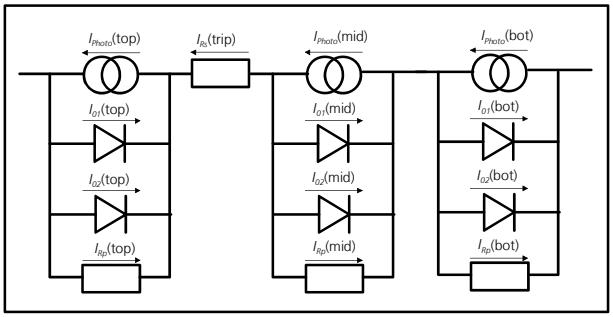

Figure 3 Equivalent network of a 3J cell. Each sub cell is described by a two diode model according to Eq. (1) where the parameters for each sub cell are derived from the component cell data.

The two diode model for a 3J (or any multi-junction) solar cell is then obtained by combining the two diode models for the component cells. The equivalent network of a 3J cell is depicted in Fig. 3. Mathematically this is done by solving the three two diode models for a given current which gives three voltages. The voltages are added up and one obtains one current-voltage pair of the 3J cell. This is repeated for a number of currents resulting in the full I-V curve of the 3J cell. It has to be noted that for the series resistance of the 3J cell the series resistance of the top component cell is used whereas the series resistances of the mid and bottom component cells are set to zero. This is justified since the major contribution to the series resistance is related to the front grid design.
Figure 4 shows some representative BOL light I-V characteristics of 3J cells and a simulated I-V curve which is the result of the combined two diode model. For each sub cell (top, middle and bottom) the input parameters were derived from fits to dark I-V curves and the measured I_{SC}'s, respectively, as demonstrated above for the top cell (Fig. 2). Again, a very good agreement between measured data and model is obtained.

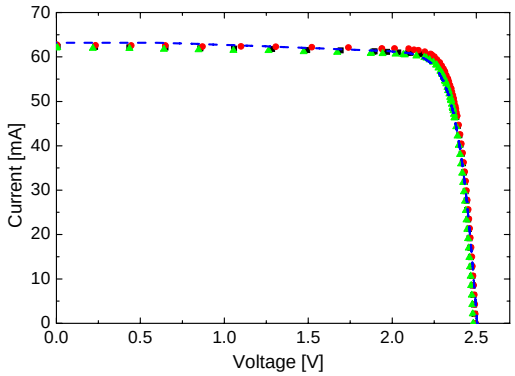

Figure 4 BOL light I-V characteristics of 3J solar cells (symbols) and a simulated I-V curve (dashed line) which is the result of the combined two diode model.

Modeling of the degradation due to particle irradiation

With regard to particle irradiation the only parameters affected in the two diode model are the two dark saturation currents I_{01} and I_{02} and the photocurrent I_{photo}.
The degradation of the dark saturation currents can be described by equations which are fully based on fundamental solar cell physics and the basic relation between irradiation fluence and lifetime of the minority carriers τ which is given by [8]:

$$\frac{1}{\tau} = \frac{1}{\tau_0} + K_\tau(n,E) \cdot \Phi \qquad (2)$$

with n being the particle type, E the energy of the particle and Φ the fluence. The particle and energy dependent quantity $K_\tau(n,E)$ is defined as the relative damage coefficient (related to the lifetime) which is proportional to the introduction rate of new defects into the semiconductor material caused by the particle irradiation.
The dark saturation currents depend on the lifetime τ in the following ways [1]:

$$I_{01} = q n_i^2 \left(\frac{\sqrt{D_e}}{N_A \sqrt{\tau_e}} + \frac{\sqrt{D_h}}{N_D \sqrt{\tau_h}} \right) \qquad (3)$$

and

$$I_{02} = \frac{\pi}{2} \frac{n_i k_B T}{\sqrt{\tau_e \tau_h}} \frac{W}{V_b - V} \qquad (4)$$

with n_i being the intrinsic carrier concentration, D and N the diffusion constant and doping concentration, W the width of the space charge region and V_b the built-in voltage. Indexes e and h refer to electrons and holes and indexes A and D refer to acceptors and donors. Inserting Eq. (2) into Eq. (3) and (4) respectively yields after some approximation the following equation for the particle fluence dependence of I_{01} and I_{02}:

$$I_{0k}(\Phi,n,E) = I_{0k}(0)\left(1+\frac{\Phi}{\Phi_0(I_{0k},n,E)}\right)^{k/2} \quad k=1,2 \qquad (5)$$

The fitting parameters $\Phi_0(I_{0k},n,E)$ are called critical fluences which are in very good approximation:

$$\Phi_0(I_{01},n,E) = \frac{1}{Max\{\tau_{e,0}K_{\tau,e},\tau_{h,0}K_{\tau,h}\}}$$
$$\Phi_0(I_{02},n,E) = \frac{1}{\sqrt{\tau_{e,0}K_{\tau,e}\tau_{h,0}K_{\tau,h}}} \qquad (6)$$

In contrast to the dark saturation currents for the photocurrent there is actually no simple equation by which its degradation can be described derived by fundamental physics. That is why for the photocurrent the following semi-empirical equation is used [1]:

$$I_{photo}(\Phi,n,E) = I_{photo}(0) - C(E)\cdot\ln\left(1+\frac{\Phi}{\Phi_0(I_{photo},n,E)}\right) \qquad (7)$$

with C being a fitting parameter defining the slope of the degradation curve. It shall be noted that Bourgoin et. al have tried to give a physical explanation for Eq. (7) [9]. However, simulation showed that the deduction in [9] only holds for a few exceptional cases and cannot be generalized.

Now, for each component cell the respective degradation characteristics for I_{01} and I_{02} according to Eq. (5) and for I_{photo}(=I_{SC}) according to Eq. (7) are derived from the respective measurements for each particle and all energies.

Figure 5 shows as an example the degradation curves of I_{01} and I_{02} of the top component cells. Symbols represent the data derived from dark I-V measurements while lines are fitting curves according to Eq. (5). While the predicted trend is perfectly met in case of I_{02} the fit of the I_{01} data is not as good. This is mostly caused by the fitting process of the dark I-V curve where I_{01} is strongly masked by R_S thus introducing a higher uncertainty to the value of I_{01}. Furthermore, it should be noted that all data points in the graphs given in Fig. 5 are derived from different top component cells which showed already differences in their dark BOL I-V characteristics.

Finally, it also should be noted that for higher fluences I_{02} becomes the dominant term in the dark I-V curve (cp. also upper graph in Fig. 2). This is a result of the fact that I_{02} increases linearly with Φ while I_{01} is only proportional to $\sqrt{\Phi}$.

Introducing now all degradation characteristics for I_{photo}, I_{01} and I_{02} for each component cell in the two diode model and combining the three two diode models according to the equivalent network shown in Fig. 3 for each particle/energy combination the corresponding 3J cell degradation curves are calculated.

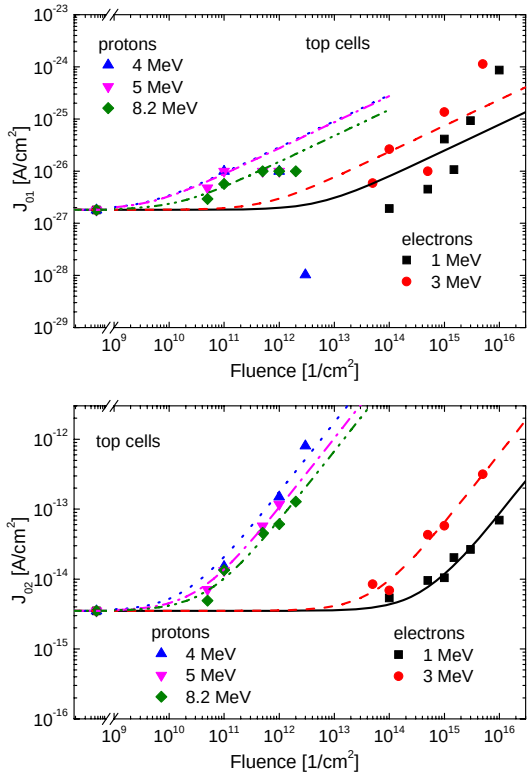

Figure 5 I_{01} and I_{02} of top component cells vs. fluence of particle irradiation of different type and energies. Symbols are data derived from dark I-V measurements, lines are fitting curves using Eq. (6).

The results are shown in Fig. 6 where the symbols represent the measured 3J cell data. Error bars to the data points are standard deviations of mean values. However, for each particle/energy/fluence combination there were typically not more three 3J cells involved in the study. The solid lines are the results of simulations using the combined two diode model. Obviously, the degradation data of the 3J solar cell can be very accurately matched by this approach.

Application of the displacement damage dose method

Since the critical fluences Φ_0 - which are reciprocal proportional to the relative damage coefficients (cp. Eq. (6)) - are dependent on the particle type and their energies, in principle, one would have to perform several irradiation tests in order to derive the energy dependence of the relative damage coefficients (or the critical fluences). And in fact, this is typically done when applying the JPL method described in [1]. However, researchers from the Naval Research Laboratory found out that the relative damage coefficients are proportional to the so-called non-ionising energy loss (NIEL) – a quantity which gives the energy transferred to the atoms in the crystal lattice of the semiconductor material as a result of several possible interactions with incident protons or electrons [2].

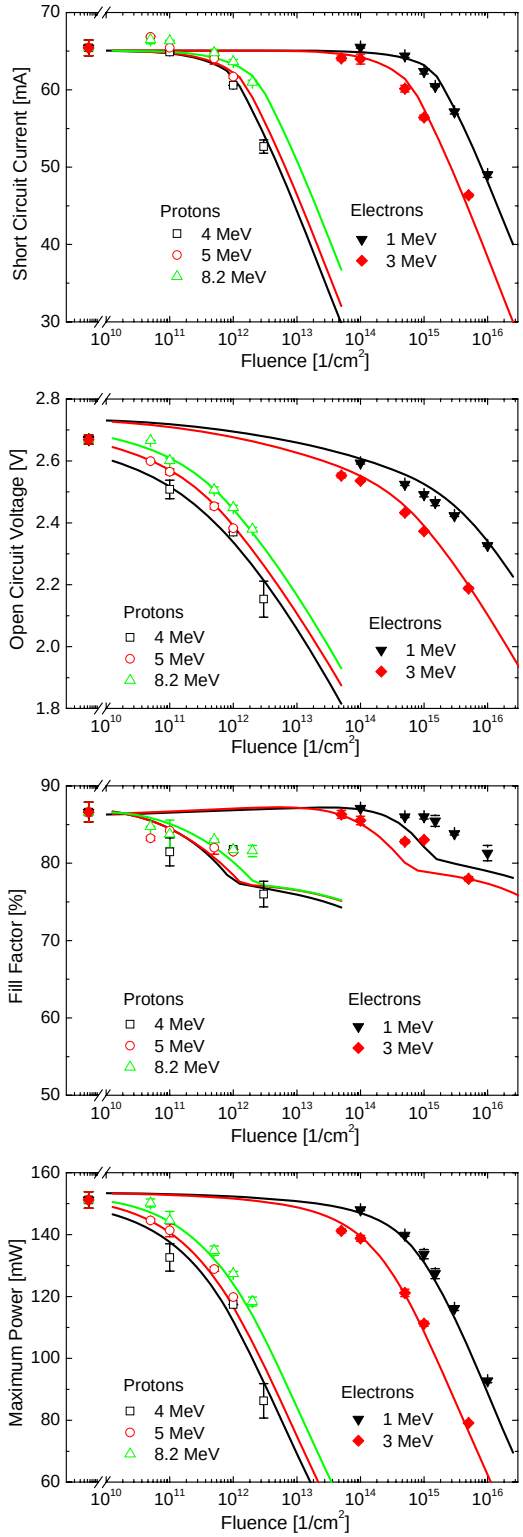

Figure 6 Degradation characteristic of the 3J cell – comparison between measured data (symbols) and simulation (solid lines).

The NIEL can be calculated using the physical laws of scattering theory (e.g. [10]). Multiplying the NIEL with particle fluences translates those into so-called displacement damage doses (DDD). As a result, the degradation curves for each particle coincide which means that the energy dependence in the degradation characteristics is cancelled out. Eq. (5) and (7) are then turned into:

$$I_{photo}(D,n) = I_{photo}(0) - C(E)\cdot\ln\left(1+\frac{D}{D_0(I_{photo},n)}\right)$$
$$I_{0k}(D,n) = I_{0k}(0)\left(1+\frac{D}{D_0(I_{0k},n)}\right)^{k/2} \quad k=1,2 \qquad (8)$$

with D_0 being the critical DDD.
The application of the DDD method to the model introduced in this paper follows the same procedure as published elsewhere [2]. However, in our case the relevant parameters to describe the degradation characteristics are I_{photo}, I_{01} and I_{02} for top, middle and bottom component cells.
In Fig. 7 the I_{02} data from Fig. 5 are plotted vs. DDD where the proton data perfectly coincides along the predicted characteristic curve. In case of the electrons the relationship between damage coefficients and NIEL is non-linear. The non-linearity is expressed by the n-factor which translates the 3 MeV doses into effective 1 MeV doses according to [2]:

$$D_{eff,e}(3\,MeV) = D(3MeV)\cdot\left[\frac{NIEL_e(3\,MeV)}{NIEL_e(1\,MeV)}\right]^{(n-1)} \qquad (9)$$

The exponent n is found by the experimental data from at least two different electron energies [2] and is in our case for the top cell 2.9. In Fig. 7 the 3 MeV electron data is plotted both vs. the "normal" dose (open circles) and effective dose (closed circles).

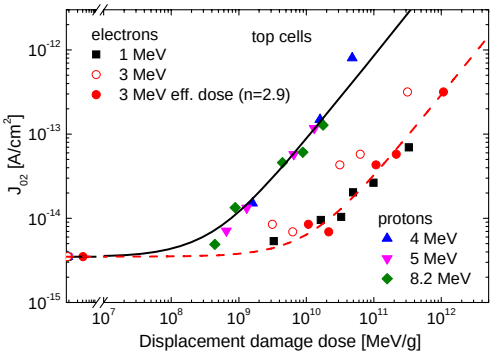

Figure 7 I_{02} of top component cells vs. DDD comparison between measured data (symbols) and simulation (solid lines).

In an analogous way the middle and bottom cell data were translated in (effective) DDDs. Finally, only the conversion

factor R_{ep} which translates electron doses in a equivalent proton doses according to [2]:

$$R_{ep}(Z) = \frac{D_{0,eff\,1MeV}(Z,e)}{D_0(Z,p)} \tag{10}$$

has to be determined for $Z = I_{photo}$, I_{01}, I_{02} and then the total dose and thus the degradation of each component cell for any given particle environment can be calculated according to:

$$D_{tot}(Z) = \int \frac{d\Phi_p(E)}{dE} NIEL_p(E)\,dE + \frac{1}{R_{ep}(Z)} \int \frac{d\Phi_e(E)}{dE} \frac{NIEL_e(E)^n}{NIEL_e(1\,MeV)^{(n-1)}}\,dE \tag{11}$$

with $d\Phi/dE$ being the particle spectra. Subscripts e and p refer to electrons and protons, respectively.
The degradation of the 3J cell is then modeled as before by combining the two diode models of the three component cells which incorporate the total doses for each sub cell. It has to be noted that total doses are in general different for each sub cell and also for each parameter since both NIEL values differ from one sub cell to another and R_{ep} values are different for each parameter I_{photo}, I_{01}, I_{02}. That is also why no graphs with 3J cell data vs. DDD are shown since strictly speaking there is no clear mapping instruction from fluence to DDD in case of multi-junction cells that are composed of different semiconductor materials. However, this does no place any restriction to the applicability of the DDD approach to the method presented here.

SUMMARY AND DISCUSSION

It has been demonstrated that component cells are quite valuable in deriving an accurate model based on fundamental solar cell physics for the performance prediction of multi-junction solar cells which are exposed to particle irradiation. The DDD approach using the NIEL values for determining the energy dependence of the relative damage coefficients can be applied without any restrictions. Even more, the DDD method is actually applied in a more correct way than is currently done elsewhere since each sub cell is treated independently. The model described here can be considered as a first step on the way to a fully consistent model of a 3J cell which also takes into account temperature effects, different sun spectra and sun intensities.
In literature it is also suggested that model parameters are accessible by measurements which can be performed only on the 3J cell (e.g. by using electroluminescence [11,12]) by which the additional testing of component cells might be avoidable. However, the simplicity of the characterization methods that need to be applied are currently considered outweighing the additional growth of component cells and irradiation tests that have to be performed on those. Finally, the model can be applied without any limitations to any multi-junction cell and does not require detailed background information about the internal cell structure. Only the semiconductor material is of relevance for applying the correct NIEL curve.

ACKNOWLEDGEMENT

The authors would like to thank Gerhard Strobl from AZUR SPACE Solar Power GmbH for providing the samples and Steve Taylor from the European Space Agency for organizing the irradiation experiments.

REFERENCES

[1] B. E. Anspaugh, "GaAs Solar Cell Radiation Handbook", JPL Publication 96-9, 1996.

[2] S. R. Messenger et al., "Modeling solar cell degradation in space: a comparison of the NRL displacement damage dose and the JPL equivalent fluence approaches", *Progr. Photovolt.* **9**(2), 2001, pp. 103-121.

[3] S. Makham et al., "Non-empirical prediction of solar cell degradation in space", *Semicond. Sci. Technol.* **20**, 2005, pp. 699-704.

[4] A. Gauffier et al., "Analytical model for multi-junction solar cells prediction in space environment", *Microelectronics Reliability* **48**, 2008, pp. 1994-1999.

[5] M. Meusel et al., "Development and production of European III-V multi-junction solar cells", *Proc. 22nd EC PVSEC*, 2007, pp. 16-21.

[6] C. Baur et al., "Investigation of Ge component cells", *Proc. 31st IEEE PVSC*, 2005, pp. 675-678.

[7] P. Würfel, "Physics of Solar Cells", WILEY-VCH, 2005.

[8] S. M. Sze, "Physics of Semiconductor Devices", Wiley-Interscience, New York, 1981.

[9] J. C. Bourgoin et al., "Irradiation-induced degradation in solar cell: characterization of recombination centres", *Semicond. Sci. Technol.* **17**(5), 2002, pp. 453-460.

[10] E. A. Burke, "Energy Dependence of proton-induced Damage in Silicon", *IEEE Trans. Nucl. Sci.*, Vol. NS-33, No. 6, 1986, pp. 1276-1281.

[11] T. Kirchartz et al., "Internal voltages in GaInP/GaInAs/Ge multijunction solar cells determined by electroluminescence measurements", *Appl. Phys. Lett.* **92**, 2008, pp. 123502-123501-123503.

[12] M. Zazoui et al., "Space degradation of multijunction solar cells: An electroluminescence study", *Appl. Phys. Lett.* **80**(23), 2002, pp. 4455-4457.